atmosphere

MDPI

Article

Predicting the Impact of Change in Air Quality Patterns Due to COVID-19 Lockdown Policies in Multiple Urban Cities of Henan: A Deep Learning Approach

Mughair Aslam Bhatti [1,2], Zhiyao Song [1,*], Uzair Aslam Bhatti [3,*] and Naushad Ahmad [4]

[1] School of Geography, Nanjing Normal University, Nanjing 210023, China; mughairbhatti@nnu.edu.cn
[2] Jiangsu Center for Collaborative Innovation in Geographical Information, Resource Development and Application, Nanjing 210023, China
[3] School of Information and Communication Engineering, Hainan University, Haikou 570100, China
[4] Department of Chemistry, College of Science, King Saud University, Riyadh 11451, Saudi Arabia; anaushad@ksu.edu.sa
* Correspondence: zhiyaosong@163.com (Z.S.); uzair@hainanu.edu.cn (U.A.B.)

Abstract: Several countries implemented prevention and control measures in response to the 2019 new coronavirus virus (COVID-19) pandemic. To study the impact of the lockdown due to COVID-19 on multiple cities, this study utilized data from 18 cities of Henan to understand the air quality pattern change during COVID-19 from 2019 to 2021. It examined the temporal and spatial distribution impact. This study firstly utilized a deep learning bi-directional long-term short-term (Bi-LSTM) model to predict air quality patterns during 3 periods, i.e., COVID-A (before COVID-19, i.e., 2019), COVID-B (during COVID-19, i.e., 2020), COVID-C (after COVID-19 cases, i.e., 2021) and obtained the R^2 value of more than 72% average in each year and decreased MAE value, which was better than other studies' deep learning methods. This study secondly focused on the change of pollutants and observed an increase in Air Quality Index by 10%, a decrease in $PM_{2.5}$ by 14%, PM_{10} by 18%, NO_2 by 14%, and SO_2 by 16% during the COVID-B period. This study found an increase in O_3 by 31% during the COVID-C period and observed a significant decrease in pollutants during the COVID-C period (PM_{10} by 42%, $PM_{2.5}$ by 97%, NO_2 by 89%, SO_2 by 36%, CO by 58%, O_3 by 31%). Lastly, the impact of lockdown policies was studied during the COVID-B period and the results showed that Henan achieved the Grade I standards of air quality standards after lockdown was implemented. Although there were many severe effects of the COVID-19 pandemic on human health and the global economy, lockdowns likely resulted in significant short-term health advantages owing to reduced air pollution and significantly improved ambient air quality. Following COVID-19, the government must take action to address the environmental problems that contributed to the deteriorating air quality.

Keywords: air quality pattern; Bi-LSTM; air pollution; COVID-19

Citation: Bhatti, M.A.; Song, Z.; Bhatti, U.A.; Ahmad, N. Predicting the Impact of Change in Air Quality Patterns Due to COVID-19 Lockdown Policies in Multiple Urban Cities of Henan: A Deep Learning Approach. *Atmosphere* **2023**, *14*, 902. https://doi.org/10.3390/atmos14050902

Academic Editor: Hung-Lung Chiang

Received: 1 April 2023
Revised: 9 May 2023
Accepted: 9 May 2023
Published: 22 May 2023

1. Introduction

In December 2019, patients with unexplained pneumonia infection were successively found in Wuhan, Hubei Province, China [1]. Experts identified the pathogen of this unexplained viral pneumonia case as a new type of coronavirus named COVID-19 [2]. As of 11 March 2020, the sickness reached every corner of the globe and was declared a pandemic. As of late March 2021, the estimated global case count was over 127 million, with over 2.7 million fatalities. The first case of infection was confirmed in Henan Province on 22 January 2020, the first-level response to major public health emergencies was launched on 24 January 2020 [3]. From 26 January, all inter-provincial and inter-city road passenger vehicles, as well as passenger through trains in the airport and the province, were suspended. Henan province implemented the measure to close all the educational institutions, including primary schools, middle schools and high schools; public transportation in the city will

be suspended one after another, communities will be managed in a closed manner, and enterprises will resume work no earlier than February. Government in China implemented strict lockdown measures in high-risk areas and middle risk areas to control the spread of COVID-19 [4].

The outbreak of the epidemic coincided with the Spring Festival in 2020. During the Spring Festival, heavy regional air pollution in Henan occurred due to high tourism and family events [5]. At present, there are three reasons for air pollution during the epidemic:

- First, the emission sources increase, e.g., fireworks and firecrackers are set off during the Spring Festival [6]. It is a subjective factor that causes heavy pollution;
- The second is the environmental capacity is greatly reduced due to unfavorable meteorological conditions. The emission of air pollutants still exceeds the environmental capacity by more than two times, and the actual emission reduction is still less than the emission reduction demand [7];
- The third is due to secondary pollution emission. During the epidemic, the emission of traffic sources was reduced, NOx was greatly reduced, the effect of ozone depletion was weakened, the proportion of NOx emission reduction exceeded Volatile Organic Compound (VOC), ozone increased significantly, and secondary particulate matter (PM) was generated especially, which offset the primary the emission reduction of pollutants.

The emission of atmospheric pollutants caused by anthropogenic activities far exceeds the environmental capacity, adverse meteorological conditions and atmospheric chemical reactions lead to the frequent occurrence of atmospheric pollution events in China's autumn and winter, and the concentration of atmospheric particulate matter (PM) and gaseous pollutants can reach several times to dozens of times the WHO recommended value [8]. Air quality and human health pose a serious threat, and so, air pollution became a hot topic of public, academic, and government concern. Gough et al. (2022) compared the air quality during the COVID-19 lockdown in China in 2020 with the 11-year average (2009–2019), and the main conclusion was: the columnar abundance of tropospheric NO_2, SO_2 and aerosol optical depth (AOD) decreased significantly, the decline of NO_2 column loads in southeast, northeast, northwest, and southwest China is quite different, and the levels of NO_2 and SO_2 in southeast and northeast China dropped significantly. Donzelli et al. [9] analyzed the concentrations of six major air pollutants in 366 cities in mainland China from 1st January to April 30th each year from 2017 to 2020. The main conclusion was that the air quality in many provinces improved significantly. Compared with the previous year, the concentration of O_3 in 2020 increased, and the national average concentrations of the other five major air pollutants all decreased; the daily variation of $PM_{2.5}$ and PM_{10} concentrations remained unchanged. Fang et al. [10] used air pollution data from 289 cities across China from 1st January 2019 to 21st February 2020, and took the first-level response to public health emergencies in 2020 as the policy time point, and used breakpoints with the regression method, the main conclusions were: the average air quality index of the city decreases by 36% under the first-level response policy, and there is urban heterogeneity: the air pollution in the cities where the process production enterprises are concentrated is more negligible, and the air pollution in the cities with denser roads is smaller. Gough et al. [11] compared the air quality during the COVID-19 lockdown in the Yangtze River Delta region with that before the lockdown, and the main conclusion was that the ambient $PM_{2.5}$ decreased. Guarnieri et al. [12] divided the Beijing–Tianjin–Hebei epidemic prevention and control into four stages: early stage, early mid-stage, middle stage, and late stage, and combined with meteorological, traffic, and industrial data, and comprehensively used mathematical statistics and spatial analysis methods. The main conclusions are: the overall AQI and six pollutants decreased compared with 2019; O_3 increased significantly in the initial stage (76.2%); the $PM_{2.5}$ concentration in Beijing in February was nearly 60% lower than that in 2014 under similar meteorological conditions; In the middle and late stages of control, the changes of various pollutants tended to be stable or slightly increased.

Hasnain et al. [13] compared the air quality in western China (Chongqing, Luzhou, Chengdu) between February 2020 (during the epidemic prevention and control period) and 2017–February 2019, and the main conclusion was that the air quality index's (three cities combined. AQI) was the highest. The average air quality indexes of the fifth day decreased by 23.6%, the average concentrations of $PM_{2.5}$, PM_{10}, SO_2, Co, and NO_2 all decreased by more than 17%, and the average concentration of O_3 increased by 6.2%. Hasan et al. [14] put southern China (Shenzhen, Guangzhou, Foshan) data from 12 January to 27 March, in 2019 and 2020 was compared with the same period in 2019. The main conclusions were: air quality index's (the combined AQIs of the three cities) decreased by 16.0%, and the average AQIs were Guangzhou > Foshan > Shenzhen in order; the top three AQIs in 2020 (2019) the distribution ratios of grades were 62.7% (45.2%), 37.3% (50.4%), and 0% (4.40%). He et al. [15] compared the improvement of air quality in Hubei Province during the COVID-19 lockdown with the improvement in air quality during the Spring Festival in 2018 and 2019, and the main conclusions were: except for NO_2, the degree of air quality improvement was lower than expected; the advancement of SO_2 was small, while the relative and absolute values of O_3 concentration increased. Wong et al. [16,17] used to work on prediction of air quality pattern during lockdown and monitor the changes.

The Need for Predicting the Impact of Lockdown Policies on Air Quality

Lockdowns were a major part of our lives since the COVID-19 pandemic hit us. Researchers studied the impact of these lockdowns on air pollution levels. They analyzed the air quality data from before and during the lockdowns to see if there was any change. Some even compared the data to a [18–20] period before the pandemic to obtain a better understanding of the impact. Interestingly, a study by Dang and Trinh [21] found that decreased variety and transit use were factors leading to improved air quality during the COVID-19 era. This suggests that reducing our daily commute and limiting travel can have a positive impact on the environment.

The research findings were not just limited to one region. Station-based data from China [22], Malaysia [23], Brazil [24], USA [25], Italy [26], and several other countries were analyzed to obtain a global understanding of the impact of lockdowns on air pollution levels [27]. Overall, these studies highlighted the potential benefits of lockdowns on air quality and the importance of reducing our daily commute and travel to improve the environment.

Changes in air quality patterns were also documented in other nations where COVID-19 cases were prevalent, and lockdowns were enacted. Hu et al. [28] examined the air quality in Croatia during the epidemic lockdown compared to 2019; The primary conclusions were that the concentrations of NO_2 and PM_{10} particles in traffic measurement points decreased by 35%, and the concentrations of total PAHs decreased by 26%; only the concentration of NO_2 in residential measurement points decreased slightly, while the concentrations of PM_{10} particles and PAHs were essentially the same as the previous year. Jakob et al. [29] compared the observed concentrations of air pollutants in Italy to the values predicted by the CAMS ensemble model (without considering lockdown measures). The average concentrations reduced by 30% and 40%, respectively, whereas the concentration of PM_{10} remained the same and the peak concentration of O_3 rose. Jakovljevic et al. [30] compared the observed concentrations of PM_{10}, $PM_{2.5}$, NO_2, and O_3 during lockdown in three medium Italian cities (Florence, Pisa, and Lucca) with the readings for the same period in 2019. In densely populated regions, there is no indication of a correlation between the deployment of lockdown measures and the reduction in particulate matter (PM) in urban centers; yet, NO_2, but not O_3, concentrations decrease dramatically. Jeong et al. [31] compared and analyzed the air quality in Southern California before and after the epidemic blockage by combining chemical weather research and forecasting model (WRF-Chem) with ground observation data. The principal results were that the population-weighted concentration of $PM_{2.5}$ reduced by 15%, and that 68% of the fall in $PM_{2.5}$ concentrations was due to emission reductions and 32% was due to meteorological changes. Karagulian et al. [32] evaluated

the mean amounts of contaminants in Victoria four weeks before and twelve weeks after a partial lockdown. The primary finding was that pollution levels were drastically lowered. Lai et al. [33] evaluated the air quality in Delhi before and after the epidemiological blockage, as well as the condition in 2019 compared to the previous year. PM_{10} and $PM_{2.5}$ concentrations reduced by more than 50 percent relative to levels before the blockage, and by around 60 percent compared to the same period in 2019. Li et al. [34] compared the air quality of Bangkok before, during, and after the lockdown to the measurements for the same time period in 2019. The concentrations of $PM_{2.5}$, PM_{10}, O_3, and CO fell dramatically, whereas NO_2 concentrations rose significantly; COVID-19 blocking actions influenced not only air pollution levels but also air pollution features.

There are two major techniques for neural networks to include context into sequence processing tasks: aggregate the inputs into overlapping time-windows and consider the job as spatial, or utilize recurrent connections to directly mimic the passage of time. The use of time-windows has two key drawbacks: first, the appropriate window size is task-dependent (too small and the network will ignore essential information, too big and it will overfit on the training data), and second, the network is incapable of adapting to shifted or time warped sequences. However, typical RNNs (that is, RNNs with buried layers of recurrently linked neurons) have their own constraints. For starters, because they analyze inputs in chronological sequence, their outputs are primarily predicated on past context (there are techniques to incorporate future context, such as inserting a delay between the outputs and the targets; however, they seldom fully use backwards dependencies). Second, they are known to struggle with learning time-dependencies that are more than a few timesteps long [35]. Bidirectional networks give an elegant solution to the first challenge. LSTM was proven to be capable of learning extended time-dependencies in the second scenario.

The spatiotemporal scale of most studies was short-term or single cities/sites, and relatively few studies were carried out on the spatial distribution, interannual variation, and seasonal and biannual variation characteristics of long-term regional pollutants. This study investigated the patterns of air quality in 18 cities of Henan province of China for five different periods, i.e., Period-2017 (the year 2017), Period-2018 (the year 2018), COVID-A (the year 2019 period which was before COVID-19), COVID-B (the year 2020 which was during COVID-19 and lockdown period), and COVID-C (year 2021 which was considered as after COVID-19 with low active cases). This study also highlighted the impact of lockdown policies on daily bases on changes in air quality patterns and highlights the changes in achievement with respect to China GB 3095-2012 ambient air quality standards with a main focus on Grade I policies standards [36,37]. Henan Province is located in central China, belonging to the area around Beijing–Tianjin–Hebei, and typical cities in northern Henan are often ranked 20th after air quality emissions [38]. Its special geographical location, topographic structure, high emission intensity and population density lead to frequent occurrences of heavily polluted weather. Henan Province implemented a number of measures for the prevention and control of air pollution, including emergency control of heavy pollution in autumn and winter. Exploring the spatio-temporal change characteristics of pollutants in different regions of Henan Province and the relationship between pollutants will help support the implementation of control policies, and so, it is essential to study the spatio-temporal change characteristics of pollutants through long-term continuous observational data. Additionally, the prediction of air quality patterns during these periods helps to implement deep learning methods for short-term and long-term relationship predictions.

2. Methods

For various reasons, predicting the influence of COVID-19 lockout rules on air quality is critical. For starters, it helps us assess how effective these regulations are at reducing air pollution. Second, it enables us to identify regions where air pollution continues to be a problem despite the adoption of these measures. These data may be utilized to perform

targeted air quality improvement actions. Finally, it can assist us in comprehending the long-term influence of these measures on air quality and informing future policy decisions.

This study is looking into the patterns of air quality in 18 cities in China's Henan province for five different years, namely Period-2017 (the year 2017), Period-2018 (the year 2018), COVID-A (the year 2019 period which was before COVID-19), COVID-B (the year 2020 which was during COVID-19 and lockdown period), and COVID-C (the year 2021 which was after COVID-19 with low active cases). Figure 1 shows the flowchart of using deep learning model for prediction of air quality patterns. This study also illustrates the influence of lockdown policies on daily basis on variations in air quality patterns, as well as changes in attainment with regard to China GB 3095-2012 ambient air quality regulations, with a particular emphasis on Grade I policies [36,37]. Henan Province is located in central China, close to the cities of Beijing, Tianjin, and Hebei. and typical cities in northern Henan are often ranked 20th after air quality emissions [38].

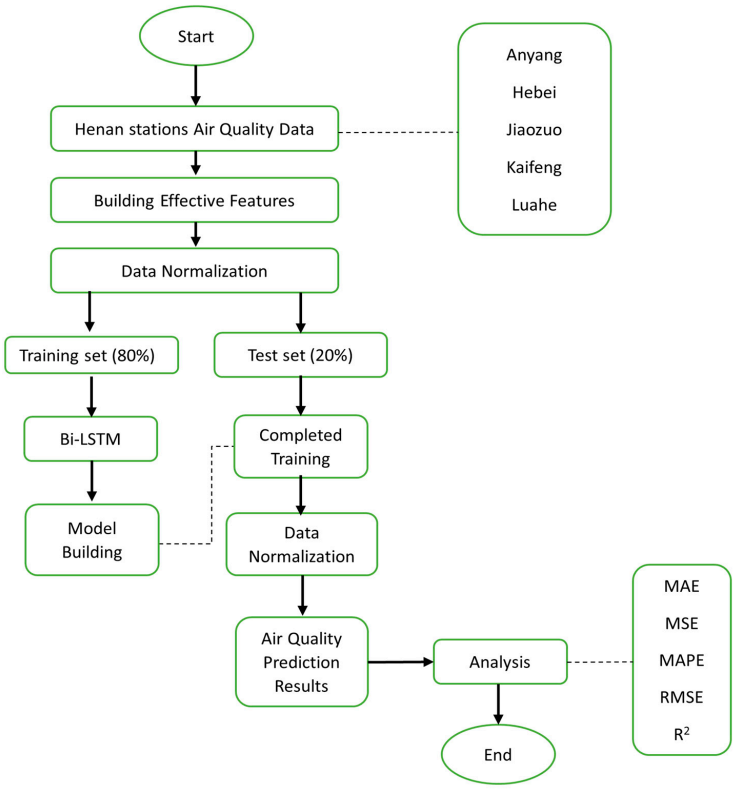

Figure 1. Flow chart for Henan Air Quality.

Because of its unique geographical location, topographic structure, high emission intensity, and population density, it experiences extremely polluted weather on a regular basis. Henan Province conducted a variety of air pollution preventive and control measures, including emergency control of severe pollution throughout the fall and winter seasons. Exploring the spatio-temporal change characteristics of pollutants in different regions of Henan Province and the relationship between pollutants will help support the implementation of control policies, and so, long-term continuous observational data are required to study the spatio-temporal change characteristics of pollutants. Furthermore, predicting air quality trends during these periods aids in the use of deep learning algorithms for short-term and long-term relationship forecasts.

2.1. Study Area Monitoring Stations

China's economy grew rapidly and is now the world's second biggest, but its economic expansion is heavily reliant on energy consumption. As a result, China became both one of the most energy-consuming and one of the most polluting countries.

Henan, a province that comprises less than 2% of the country's territory yet feeds around 7.5% of the people, emerged as an important economic province in China. Henan's economy also advanced rapidly in recent years, with GDP reaching 4.4 trillion yuan in 2017. However, its economic development is mainly reliant on the use of fossil fuels, which causes severe pollution and high emissions.

Henan is one of the world's oldest areas, as well as one of the most important original places of the Chinese nation and civilization. The compass, papermaking, and gunpowder were all created in Henan, one of the four major innovations of ancient China. Throughout history, more than 20 dynasties (spanning over a thousand years) established their capitals in Henan, making it the province with the most ancient capitals in China.

Henan also offers a plethora of tourism resources, as well as several cultural artifacts and historical places. Henan possessed six global cultural heritage sites (compared to China's 37), 358 major cultural relics under national protection, and 13 national tourist attractions as of 2017. As a result, Henan is a world-renowned cultural tourism destination. Henan Province received 665.11 million tourists in 2017, with 3.0732 million of them being overseas visitors [39].

The China includes the province of Henan, usually known simply as "Henan". Zhengzhou, the capital of the province, is situated in the middle of China [40]. Henan Province is located between 31°23′–36°22′ north and 110°21′–116°39′ east, linking Anhui and Shandong to the east, Hebei and Shanxi to the north, and Shaanxi to the west, south of Hubei. The south of Henan Province is subtropical. It has a continental monsoon climate that transitions from subtropical to temperate. East to west, the environment changes from plain to hilly and mountainous. Frequent, complex weather catastrophes occur. The province's annual temperature from south to north is 10.5–16.7 °C, the average annual precipitation is 407.7–1295.8 mm, the most significant rainfall occurs in June–August, the yearly average sunlight is 1285.7–2292.9 h, and the annual frost-free period is 201–285 days. All stations used in this are stationary stations and no other mobile stations are used in this study. Figure 2 shows Henan Province with the selected cities and station details are present in Supplementary Table S1.

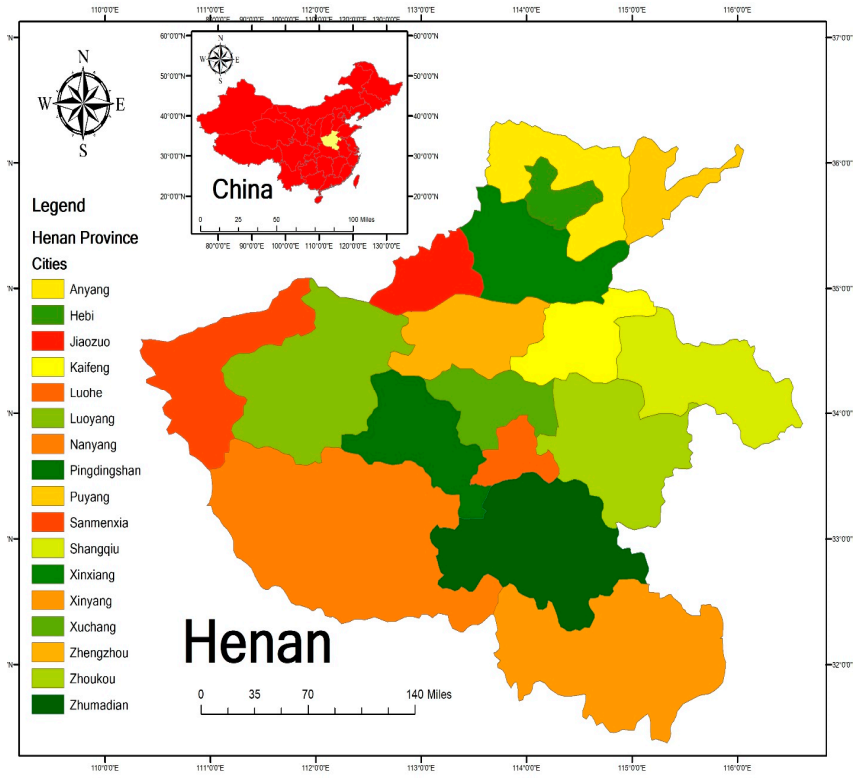

Figure 2. Study Area with selected cities.

2.2. Air Pollutant Data

Air pollution data from many sites were daily averaged for use in this article. From the weather forecast website [41], we obtained the mass concentration data necessary to calculate the AQI and the ambient air pollutants ($PM_{2.5}$, PM_{10}, SO_2, NO_2, CO, and O_3). The ambient $PM_{2.5}$, PM_{10}, NO_2, CO, SO_2, and O_3 concentrations were recorded hourly at each monitoring station, and then, the daily average for each city was calculated. Data for five years were considered from 1st January to 30th August due to better comparison with the year 2020 due to high COVID-19 cases recorded during this period.

2.3. Long-Term Short-Term Memory (LSTM) Model

For the prediction of yearly pollutants, the LSTM model mainly consisted of two LSTM units for learning spatiotemporal evolution features [42]. The LSTM unit is a module consisting of repeating grids, each grid consisted of 3 important gates, namely forget gate, the input gate, and output gate [43]. The forget gate, labeled f_t, controls the memory function of the network and can be expressed (shown in Figure 3) as:

$$f_t = \sigma\left(W_f[h_{t-1}, X_t] + b_f\right) \tag{1}$$

where σ represents the sigmoid function, which can be written as:

$$\sigma(x) = \frac{1}{1 + e^{-x}} \tag{2}$$

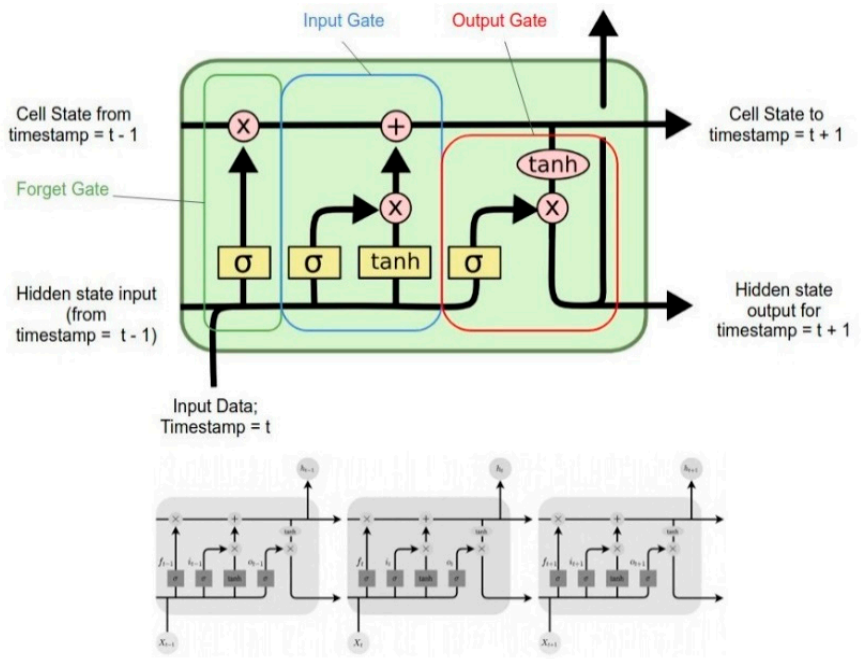

Figure 3. LSTM gates processing.

In addition, h_{t-1} represents the output of the previous grid, X_t represents the input value of the current shed, and W_f and b_f represent the weight and bias values, respectively. The input gate i_t is another important gate, and has a similar form to the forget gate f_t:

$$i_t = \sigma(W_i[h_{t-1}, X_t] + b_i) \tag{3}$$

In the formula, W_i and b_i represent the weight and bias values, but these values differ from the values of the forget gate. The candidate value c' can be expressed as:

$$C'_t = \tan h(W_{c'}[h_{t-1}, X_t] + b_{c'}) \tag{4}$$

This study chooses the tanh function instead of the sigmoid function as the excitation function.

When it comes to creating complex neural networks, choosing the right activation functions is crucial. Two popular functions that were extensively used are tanh and sigmoid. Both functions are monotonically increasing and asymptote at some finite value as the input approaches positive or negative infinity. Interestingly, tanh is a type of sigmoid function, known as the hyperbolic tangent function. Despite their similarities, there are a few key differences between the two functions. Sigmoid values range between 0 and 1, while tanh values range between 1 and −1 [44]. Additionally, the tanh function is symmetrical about the origin, which makes it ideal for normalizing inputs and producing outputs that are on average close to zero leading to faster convergence. This is important because it helps to prevent the exploding gradient problem, where the value of the gradients becomes very large. Overall, the use of tanh as an activation function can help to create complex neural networks that are both stable and effective. The gradient behavior of the two functions is a significant distinction [45]. Tanh's gradient is four times larger than the sigmoid function's gradient. This means that utilizing the tanh activation function leads in greater gradient values during training and higher updates to the network's weights. So, we utilize the tanh activation function if we want strong gradients and large learning steps [46].

C_t means that the state of the current shed is updated, and the previous state C_{t-1} will also affect the state of the current grid. The process can be expressed as:

$$C_t = f_t^* C_{t-1} + i_t * C_t' \tag{5}$$

Since the current grid state was updated, the output value o_t can be calculated, and the parameter h_t in the next grid can be obtained. The following formula can be obtained:

$$o_t = \sigma(W_o[h_{t-1}, X_t] + b_o) \tag{6}$$

$$h_t = o_t \, ^* \tan \mathrm{h}(C_t) \tag{7}$$

2.4. Statistical Analysis

This study focused on better understanding how COVID-19 impacted air quality in the surrounding area. Therefore, we analyzed the six air pollutants of Period-2017 (year 2017), Period-2018 (year 2018), COVID-A (the year 2019 period which was before COVID-19), COVID-B (year 2020 which was during the COVID-19 and lockdown period), and COVID-C (the year 2021 which was considered as after COVID-19 with low active cases). Because seasonal variations in air pollution are more significant than annual ones, the year 2019 was selected as the COVID-A period so that we could compare all four seasons rather than simply winter [47]. It was determined by comparing 2017 (Period-2017) and 2018 (Period-2018) results that the changes had a significant impact on air pollutant trends. The data were statistically analyzed using SPSS (version 25; IBM Company). The minimum and maximum values at each monitoring station, as well as the mean, median, and standard deviation (SD), were used to define the amounts of ambient air pollutants since they all followed a normal distribution. Additionally, we monitored the daily average variation in air pollutant concentrations during COVID-19's operation in an effort to identify patterns. Plotting and analysis were carried out in OriginPro 2021, while the Seaborn library was used for visualization. Maps depicting regional variations in air pollution levels were also generated using the geographic information system ArcGIS.

3. Results

Results in this study highlight the patterns of air quality among different cities spatially, daily, and yearly in the province.

3.1. City-Wise Change in Air Quality Patterns

Change of pollutant concentration was observed in different cities of Henan province and shown in Figure 4 and Table S2. $PM_{2.5}$ was recorded lowest during the COVID-C period and an average decrease in percentage was observed in Anyang city, which was −56% and concentration decreased to 29.78 $\mu g/m^3$ from 67.09 $\mu g/m^3$. Other cities recorded a decrease in $PM_{2.5}$ such Hebi by −45%, Jiaozuo by −49%, Kaifeng by −49%, Luohe by −51%, Luoyang by −51%, and Nanyang by −52%. A similar decrease in PM_{10} was observed in almost all cities during the COVID-C period, in which the highest decrease of almost −40% was observed in Nanyang, Xinyang, ZhuMaDian, and Zhengzhou. The main sources of urban particulate matter include urban dust sources, coal combustion sources, direct emissions from processes, traffic sources [48], and secondary sources, as well as other sources such as biomass combustion, cooking fume, and sea salt particles [49]. In addition, the above-mentioned sources can be further subdivided, such as dust sources can be further subdivided into urban dust, road dust, construction dust, etc.; coal-fired sources can be divided into industrial boiler coal, power plant coal, civil coal, etc.; traffic sources can also be subdivided into gasoline locomotives, diesel locomotive sources, etc. Secondary sources can be subdivided into secondary sulfates, secondary nitrates, and secondary organics [50]. Secondary sources were not directly emitted through emission sources, but gaseous pollutants such as SO_2, NOx, and volatile organic compounds emitted from emission sources such as factories and motor vehicles produce secondary aerosols through photochemical reactions and liquid-phase reactions called the secondary source. The decrease in the COVID-C period was due to the policy implementation of control of pollution by the Henan government and addressing both the symptoms and root causes [51], by highlighting industrial pollution control and emission reduction, resolutely eliminating outdated production capacity, drastically reducing coal-fired pollution, and paying close attention to diesel truck pollution [52]. Promoted VOCs management, actively responded to heavy pollution weather, rectified, and banned more than 120,000 "scattered and polluting" enterprises in the province, cleared coal-fired boilers under 35 tons of steam and coal-fired power units in the main urban areas of Zhengzhou, Luoyang, and other cities [53].

Similar changes were observed for NO_2 and O_3 where the ozone concentration decreased much in different cities; the maximum decrease was observed in Jiyuan, Zhoukou, Xinyang, Puyang, Luohe, Anyang, and Jiaozuo, where a 50% decrease was recorded in the COVID-C period. An increase in Ozone (O_3) was observed with the maximum increase in Anyang, Hebi, Kaifeng, Luoyang, and Sanmenxia record an increase of more than 60% in the COVID-C period. Since the outbreak of the new crown epidemic in early 2020, many countries around the world successively issued social distancing policies [54]. The reduction in human activities not only stopped the epidemic, but also brought unexpected benefits: the noise was significantly reduced, wild animals came out to wander, and even the air pollution index was greatly reduced. The ozone (O_3) layer, which is more than 20 km from the biosphere, is a region of the stratosphere in which oxygen and ozone molecules are constantly being converted back and forth. Pollution of the ozone layer is widespread because it forms in the lowest layer of the atmosphere, the troposphere, and then spreads through the air we breathe. Chemical interactions between nitrogen oxides (NOX) and volatile organic compounds (VOCs) under sunlight are the primary source of ozone pollution in the troposphere, especially during the clear and overcast late spring, summer, and fall. Ozone in the atmosphere's upper layers is very corrosive [55]. Ozone (O_3) molecules only differ structurally from oxygen molecules by one oxygen atom (O_2). Ozone, however, is quickly broken down at normal temperature because this form of oxygen is so unstable. Strongly oxidizing oxygen atoms are produced during ozone breakdown, which may not only demolish cell membranes and inactivate proteins but also degrade DNA and RNA and assault cells from all directions [56].

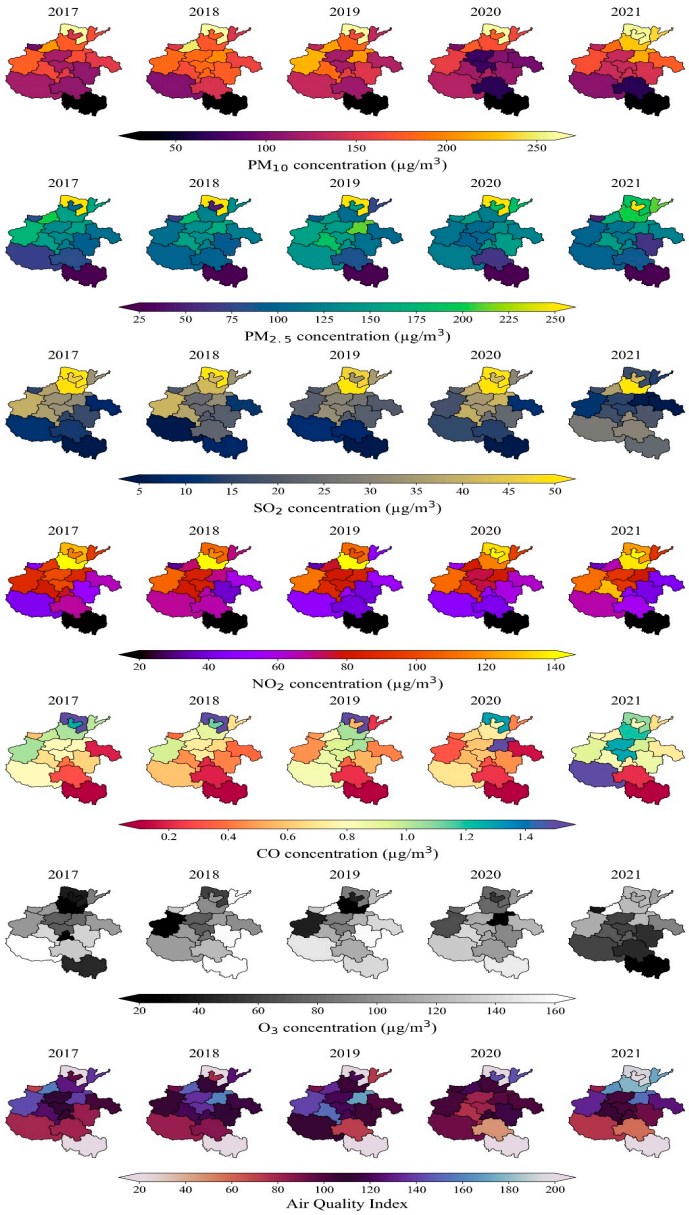

Figure 4. City-wise change of air quality patterns in Henan.

Ozone is a potent irritant that, at high enough concentrations, may cause premature skin aging and mortality and respiratory disorders that affect the mucous membranes lining our eyes and airways. Unlike particulate pollutants such as $PM_{2.5}$, ozone is a tiny air molecule difficult to block with standard face masks. Therefore, the most cost-effective way to deal with ozone pollution is not "prevention", but "hide". The ozone generation is inseparable from light, and so, ozone pollution is mainly concentrated in the afternoon of spring and summer. However, because it is easily degraded, we can avoid most of the ozone damage as long as we avoid traveling during the peak period of ozone pollution and reduce the frequency of opening windows for ventilation during this period [57].

3.2. Provincial Change Analysis

During the COVID-C period, CO was changed by −58.36%, NO_2 was changed by −89.47%, O_3 was changed by 31.25%, PM_{10} was changed by −41.69%, $PM_{2.5}$ was changed by −96.55%, and SO_2 was changed by −35.77%. Ozone increases when NOx concentration in human emissions decreases, the reduced NO concentration makes the rate of ozone decomposition slower. Moreover, during the isolation period, the increase in human activities

in courtyards and gardens is very likely to lead to an increase in the concentration of VOCs and promote the accumulation of ozone. This same type of results were highlighted by different studies globally [58,59]. During the COVID-B period, CO was changed by 9.55%, NO_2 was changed by −13.8%, O_3 was changed by −5.06%, PM_{10} was changed by −17.97%, $PM_{2.5}$ was changed by −14.18%, and SO_2 was changed by −15.78. During COVID-A, CO was changed by −21.73%, NO_2 was changed by −8.81%, O_3 was changed by −3.97%, PM_{10} was changed by −10.74%, $PM_{2.5}$ was changed by −3.36%, and SO_2 was changed by −32.79%. In Year−2018, CO was changed by −21.45%, NO_2 was changed by −8.27, O_3 was changed by 5.41%, PM_{10} was changed by −5.17%, $PM_{2.5}$ was changed by −7.11%, and SO_2 was changed by −44.98%. The reasons for these control in pollutants pattern was due to the prevention and control of air pollution, the incorporation, prevention, and control of air pollution into national economic and social development planning, urban and rural planning, optimize industrial structure and layout, the adjustment of energy structure, promotion of clean energy utilization, and reduction in coal consumption. Henan government implemented different policies to gradually reduce the discharge of air pollutants, establish and improve the coordination mechanism for air pollution prevention and control, and urge relevant departments to perform their supervision and management duties in accordance with the law. Figure 5 shows the change of air quality patterns in Henan Provinces in the last 5 years. Table 1 shows the detailed change of air quality pattern in province.

Table 1. Change of air quality pattern in Henan during COVID-19.

Year	Method	Statistical Analysis of Air Pollutants							Mean Change from Last Year (%)					
		AQI	CO	NO_2	O_3	PM_{10}	$PM_{2.5}$	SO_2	CO	NO_2	O_3	PM_{10}	$PM_{2.5}$	SO_2
2021 COVID-C	Max	378.71	1.91	71.43	200.21	691.21	170.57	27.08	−58%	−89%	31%	−42%	−97%	−36%
	Min	14.15	0.10	1.67	28.00	4.57	1.09	1.00						
	Mean	56.73	0.61	15.21	97.54	60.11	26.62	6.91						
	Std	27.18	0.20	7.11	30.27	44.94	13.28	3.32						
	Median	52.13	0.60	14.08	92.81	48.52	24.38	6.42						
2020 COVID-B	Max	452.13	24.00	103.71	214.84	443.04	429.46	48.83	10%	−14%	−5%	−18%	−14%	−16%
	Min	13.63	0.11	3.25	3.00	4.60	2.93	1.13						
	Mean	81.89	0.97	28.82	67.06	85.17	52.33	9.39						
	Std	45.79	1.79	14.81	32.34	47.15	40.05	4.95						
	Median	69.75	0.76	25.63	65.83	75.29	38.88	8.38						
2019 COVID-A	Max	483.43	5.58	117.17	205.13	508.83	496.14	75.94	−22%	−9%	−4%	−11%	−3%	−33%
	Min	14.17	0.10	2.08	1.00	5.08	2.75	1.00						
	Mean	93.02	0.88	32.79	70.46	100.48	59.75	10.87						
	Std	54.36	0.46	16.45	38.15	59.13	48.56	6.35						
	Median	76.13	0.78	29.50	67.87	85.59	41.95	9.42						
2018	Max	441.18	5.48	135.00	219.21	559.67	412.05	134.38	−21%	−8%	5%	−5%	−7%	−45%
	Min	13.86	0.13	2.75	1.00	7.64	3.19	1.00						
	Mean	96.72	1.07	35.68	73.26	111.27	61.75	14.43						
	Std	55.25	0.49	17.30	37.80	69.52	46.58	8.64						
	Median	80.60	0.96	32.50	69.58	91.92	47.46	12.58						
2017	Max	472.58	12.87	155.75	249.88	656.71	439.88	443.00						
	Min	13.29	0.13	2.05	1.00	4.29	1.62	1.00						
	Mean	100.06	1.30	38.63	69.29	117.02	66.14	20.93						
	Std	56.41	0.74	18.93	37.96	69.10	48.11	15.05						
	Median	85.24	1.14	35.83	62.70	102.09	51.96	17.48						

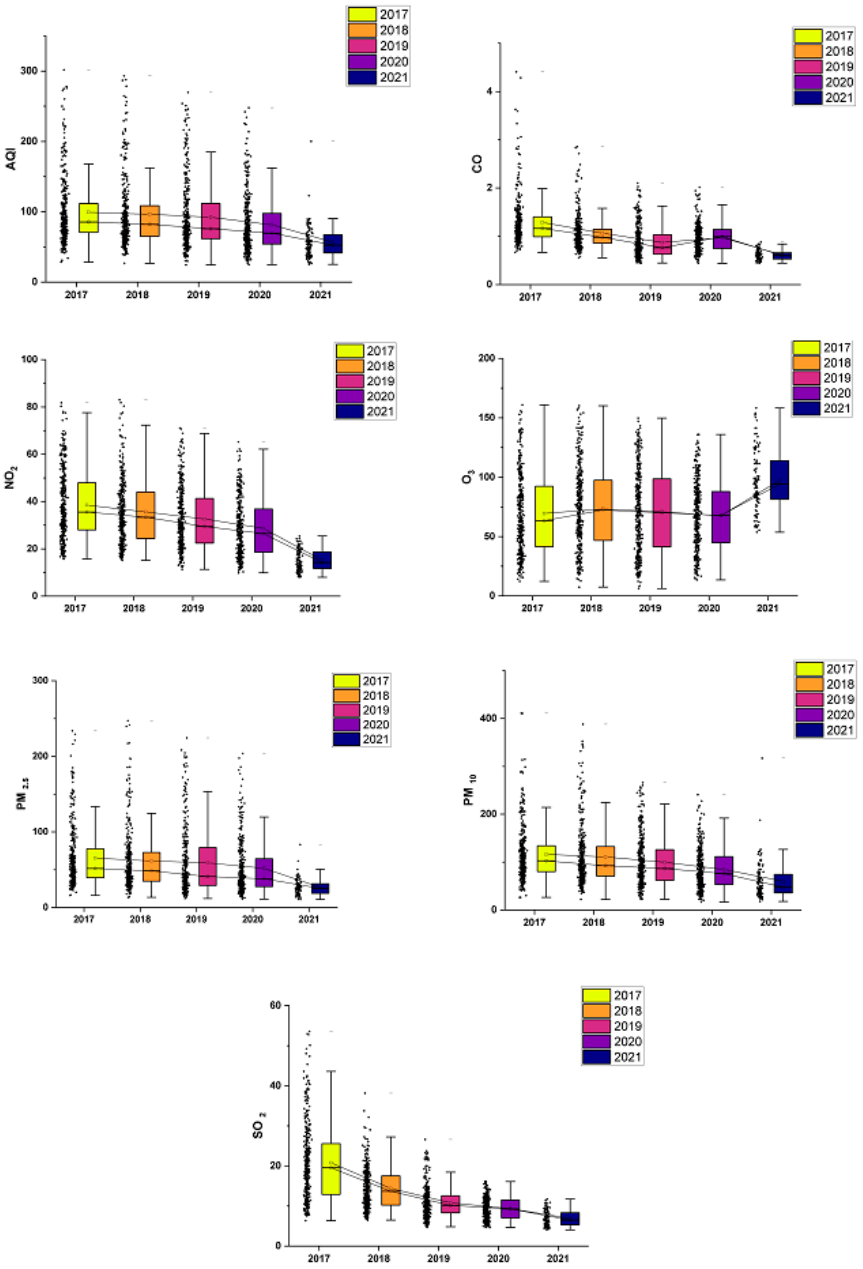

Figure 5. Provincial changes in air quality pattern in Henan.

3.3. Change of Air Quality Pattern Due to Lockdown

The world, especially urban areas, recorded a sharp drop in air pollutant emissions last year amid lockdowns and related travel restrictions due to the COVID-19 pandemic [60]. Similarly, an impact was observed in Henan after reporting the first case of COVID-19 on 24 January. The government implemented the lockdown in different cities between 24 January 2020 and 6 April 2020, with various restrictions of movement. During this period, AQI level achieved the world AQI standard [61], of good air quality with values mostly lower 60 during post lockdown period. PM_{10} and $PM_{2.5}$ observed a similar reduction in concentration during the post lockdown period and $PM_{2.5}$ and PM_{10} achieved values between 10 $\mu g/m^3$ and 50 $\mu g/m^3$ during this period which is under the same standard of China [62] of Grade I. After the relaxation of lockdown policies by the government, the concentration of pollutants crossed the Grade II level again, which shows the COVID-19 restrictions significantly impacted air quality. Low population density, low consumption of coal, reduced density, and low traffic made a better impact on particulate matter ($PM_{2.5}$ and

PM_{10}) reduction. SO_2 did not observe much change during the COVID-19 lockdown period, while NO_2 observed a drop (25 $\mu g/m^3$ to 35 $\mu g/m^3$) after lockdown but an increase after October 2020 when lockdown policies were reduced. Sulfur dioxide (SO_2) and nitrogen dioxide (NO_2) pollutes the air mainly due to the burning of fossil fuels in transportation and industrial processes. Nitrogen dioxide is a brown-red toxic gas with a pungent odor. It will have a significant impact on the human body [63]. After exposure to nitrogen dioxide above 150 mg/m^3 for 3 to 24 h, the human respiratory tract will experience discomfort, including symptoms such as cough, fever, shortness of breath, bloodshot sputum, extreme weakness, nausea, and headache. In addition to damage to the human respiratory tract, nitrogen dioxide harms water, soil, and the atmosphere. COVID-19 proved to be an unplanned experiment in air quality that did lead to temporary local improvements [64]. However, a pandemic is not a substitute for sustained and systematic action to deal with major drivers of population and climate change, thereby protecting the health of people and the planet. Changes in air quality patterns due to lockdown policies are shown in Figure 6.

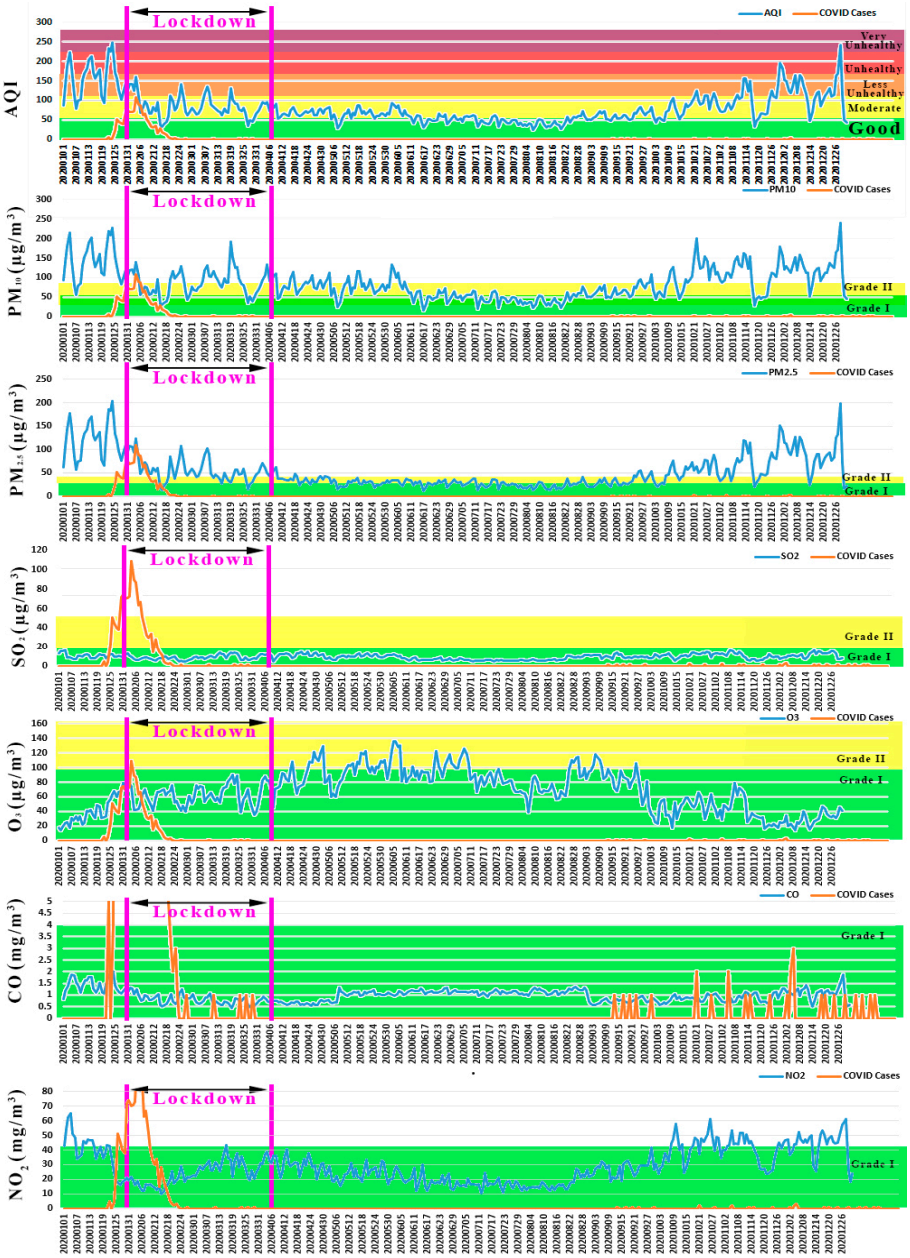

Figure 6. Change of air quality patterns due to lockdown implementation.

3.4. Prediction Pattern of Air Quality Patterns in 5 Years

This paper studied the LSTM model, which performed best in predicting air pollution concentrations in the Henan province's multiple cities (Figure 7). LSTM predicted PM_{10} and $PM_{2.5}$ with R^2 values of 0.67 and 0.67, RMSE values of 11.41 and 6.66, and MAE values of 6.89 and 6.11, respectively, throughout the COVID-19 (COVID-B) period. Among other pollutants, the projected R^2 values using LSTM for SO_2, NO_2, CO, and O_3 were 0.63, 0.54, 0.69, and 0.71, respectively, with RMSE values of 0.87, 6.10, 0.14, and 7.12 and MAE values of 0.81, 4.12, 0.07, and 5.71. Similar work was carried out by using [65], which took the prediction of daily concentrations of a variety of ground-level air pollutants into account. These ground-level air pollutants include CO, PM_{10}, NOx, SO_2, and O_3, and they were measured by an ambient air quality monitoring station in Ghadafan village in Oman. The models were trained using the multi-layer perceptron (MLP) approach in conjunction with the Back-Propagation (BP) algorithm. The findings demonstrate that there was a very excellent agreement between the anticipated and actual concentrations, as the values of the coefficient of multiple determinations (R^2) for all ANN models were more than 0.70. These values of R^2 were almost near to our proposed methods for different air quality pollutants of the COVID-B period. The findings also demonstrated that temperature has a major influence on daily changes of O_3, SO_2, and NOx, while wind speed and direction play important roles in daily variations of NO, CO, and NO_2. The concentrations of PM_{10} were affected by practically all of the meteorological conditions that were monitored.

Furthermore, during the COVID-C period, LSTM predicted PM_{10} and $PM_{2.5}$ concentrations with R^2 = 0.64 and 0.67, RMSE = 19.21 and 8.10 and MAE = 12.11 and 9.01, respectively (Figure 8). This shows that during the COVID-C period, performance of the LSTM method performed better with low RMSE and MAE values. LSTM predicted SO_2 concentration with R^2 = 0.61, RMSE = 0.79, and MAE = 0.69, NO_2 concentration with R^2 = 0.59, RMSE = 4.92, and MAE = 3.98, CO concentration with R^2 = 0.70, RMSE = 0.07, and MAE = 0.12, and O_3 concentration with R^2 = 0.65. The model performed well in predicting SO_2 concentrations during the COVID-C period, whereas the R^2 value of LSTM was greater for NO_2 prediction during the COVID-B and lowered during the COVID-C, although the RMSE value was lower during the COVID-C. For $PM_{2.5}$ forecasting, [66] created a hybrid model using feature selection and a support vector machine (SVM). First, a feature selection method based on linear causality was proposed to discover the causality between features and select the features with strong causality, thereby eliminating the redundant features in air pollution data and lowering the workload of data analysis, with the goal of determining the impact of meteorological factors on $PM_{2.5}$. This hybrid method also achieved the R^2 of more than 0.50 for particulate matter on different datasets, the same as our developed method. By combining the strengths of the principal component regression (PCR) model, the support vector regression (SVR) machine, and the autoregressive moving average (ARMA) model, Liu et al. developed an air quality prediction model that greatly improved the accuracy with which six different types of air pollutants can be predicted. A principal component analysis was first used to extract the most important information about the elements influencing air quality, and then, principal component regression was used to forecast the concentrations of six different pollutants. This hybrid method also achieved the R^2 of more than 0.5 for different pollutant concentrations [67].

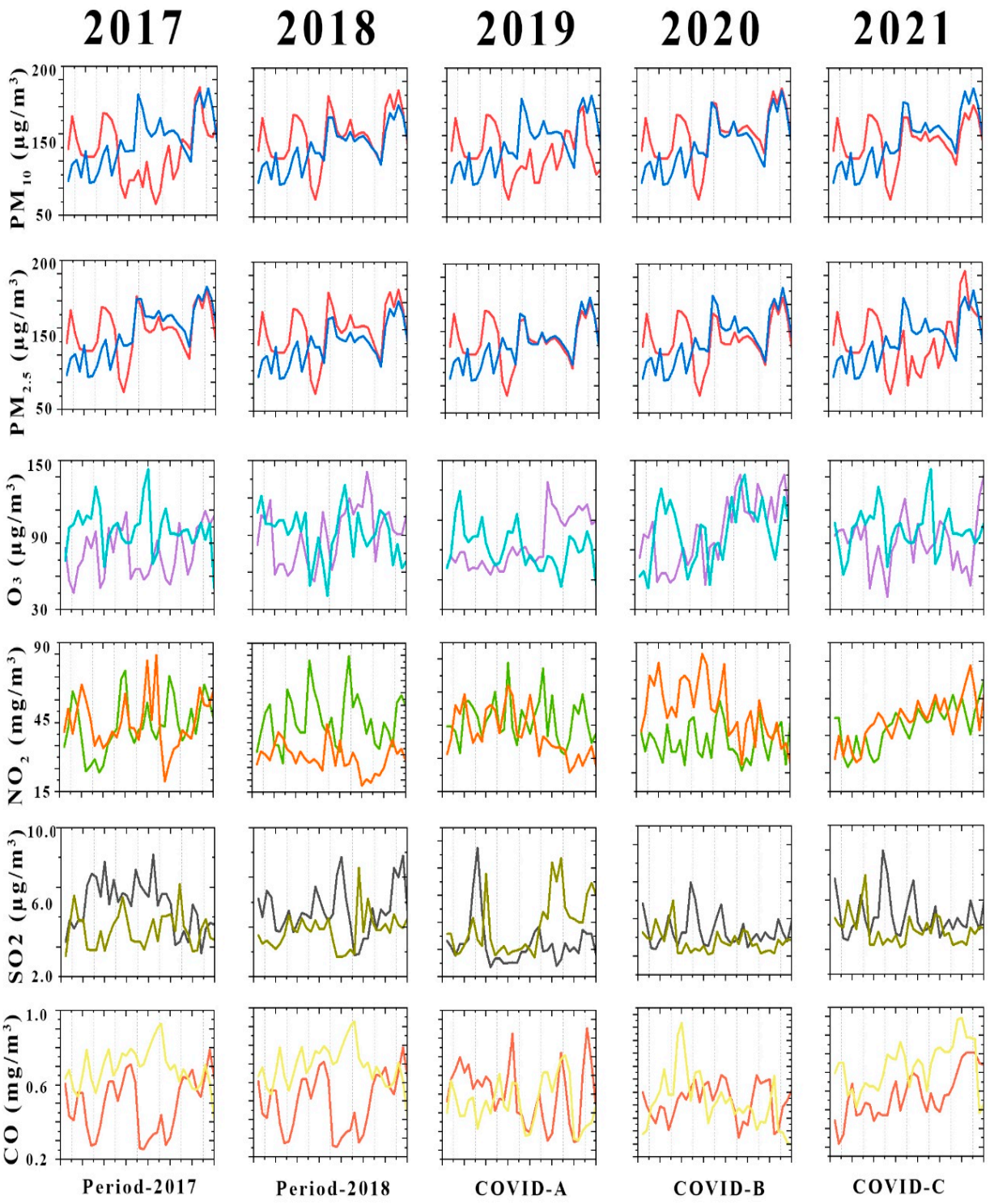

Figure 7. Actual vs. predicted values for 5-year change of air quality pollutants (x axis legends are days from 1 to 150 days).

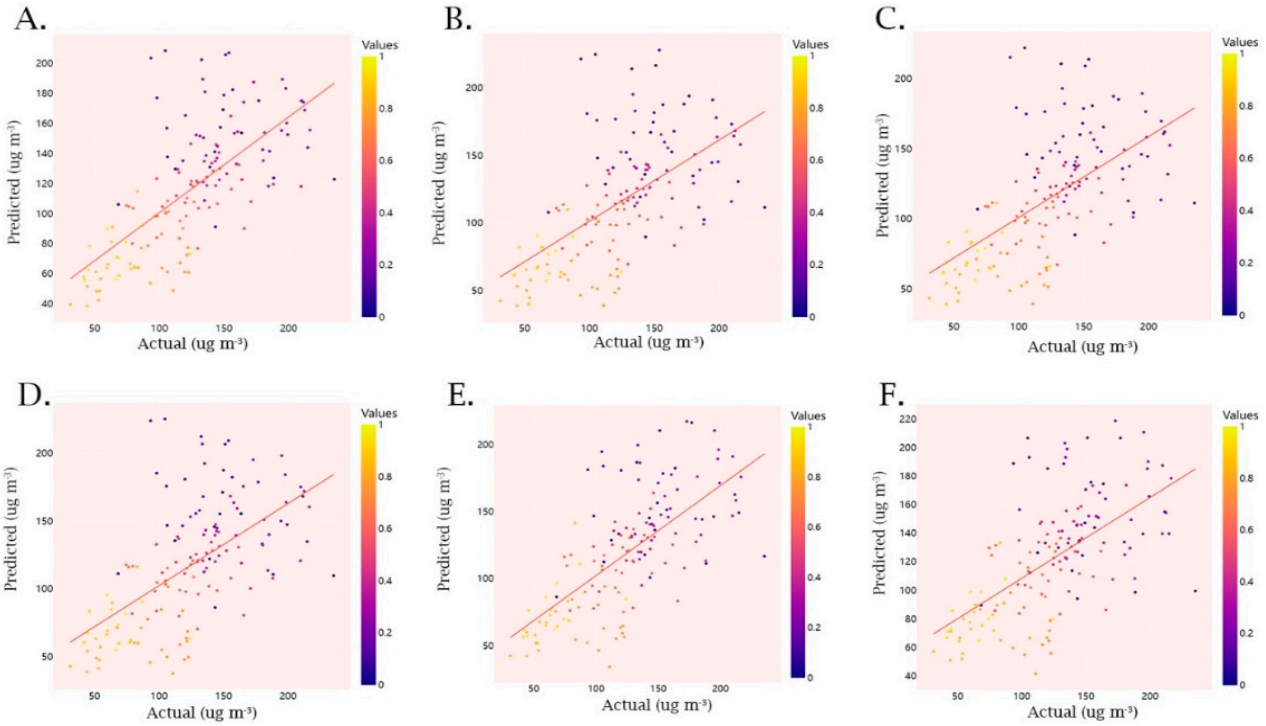

Figure 8. Actual vs. predicted comparison of particulate matter during COVID-19 (**A**) $PM_{2.5}$ COVID-A (**B**) $PM_{2.5}$ COVID-B (**C**) $PM_{2.5}$ COVID-C (**D**) PM_{10} COVID-A (**E**) PM_{10} COVID-B (**F**) PM_{10} COVID-C.

4. Discussion

Predicting the impact of COVID-19 lockdown policies on air quality is important for several reasons. Firstly, it helps us understand the effectiveness of these policies in reducing air pollution. Secondly, it allows us to identify areas where air pollution remains high despite the implementation of these policies. This information can be used to implement targeted measures to improve air quality. Finally, it can help us understand the long-term impact of these policies on air quality and inform future policy decisions. The COVID-19 pandemic had a profound impact on the world, and one of the unforeseen consequences was the improvement in air quality in many cities as a result of lockdown policies. However, it is important to understand the extent to which these policies are effective in reducing air pollution, and also to identify areas where air quality remains a concern despite the implementation of these policies. This information can then be used to develop targeted measures to improve air quality in these areas. Several studies worked on spatiotemporal analysis [68], change of haze [69,70], and carbon emission [71] which can use the deep learning model to extend the prediction to future.

Our study results are similar to a recent study [72] which sought to evaluate the behavior of the most polluting cities in the world by comparing a typical week before quarantine to an atypical week during quarantine. The study considered the relationship between population and air quality stations, with developed countries having a higher number of stations per inhabitant than emerging countries. However, the lack of access to data on air pollution in emerging countries, where public and private transport systems are high, can cause errors or alterations in the real information on the state of air quality. Another study [73] aimed to build a deep learning time series model using the Bi-directional Long Short-Term Memory (Bi-LSTM) network, combining various factors such as AOD, meteorology, and socio-economic factors. However, our study is an extended work which focused on multiple cities and the analysis of the behavior of air quality patterns. Aamir et al., [1] in his work, highlighted the spatial change in air quality without using the prediction model, which our study added. Bhatti et al. [3] focused on Jiangsu to study the spatiotemporal variation of air quality during COVID-19 and before COVID-19; however,

that study can also be improved if results use deep learning methods. Hasnain et al. [13] focused on the lockdown period to monitor the air quality and pollution change, but deep learning method was not used, whereas our study used the deep learning method.

Recently, many researchers focused on using deep learning for air pollutant concentration prediction, each taking a unique approach to the subject matter [74–80]. Bai et al. [81] comprehensively reviewed various prediction methods, ranging from statistical, artificial intelligence, numerical, and hybrid models, presenting their respective advantages and disadvantages. Meanwhile, Masih et al. [82] undertook a survey of machine learning techniques specifically for air pollutant concentration prediction, emphasizing the importance of input predictors, geographic location, and machine learning techniques such as linear regression, neural network, support vector machine, and ensemble learning algorithms. Cabaneros et al. [83] focused on the use of artificial neural networks for long-term prediction of outdoor pollutants, highlighting the predominant use of meteorological and source emissions predictors. Liao et al. [84] provided a brief review of deep learning methods for air pollution prediction, introducing the use of deep network architectures to explore non-linear spatio-temporal correlations across multiple scales of air pollution. Finally, Masood and Ahmad [85] presented an overview of AI-based methods commonly used for air pollution prediction, discussing the technological gaps and the strengths and limitations associated with different AI techniques. Despite the thoroughness of these studies, there is still a demand for an overarching and comprehensive review on air pollutant concentration prediction.

As technology advances, so too does our ability to predict air pollutant concentrations. A plethora of algorithms emerged, falling into two distinct categories: non-deep learning methods and deep learning methods. The non-deep learning methods can be further subdivided into deterministic and statistical models, each with their own strengths and weaknesses [82]. The deterministic models, such as the Community Multiscale Air Quality (CMAQ) model [83] and the Nested Air Quality Prediction Modeling System (NAQPMS) [86], rely on pre-determined equations to make predictions. Meanwhile, the statistical models, such as the Comprehensive Air-quality Model with extension (CAMx) and the Weather Research and Forecasting/Chemistry-Madrid (WRF/Chem-MADRID) [85], use data analysis to identify patterns and make predictions. However, even with these models, there are limitations. For example, the use of ideal theory in determining the model structure and the estimation of parameters based on experience can hinder their predictive performance [87]. Despite these limitations, the continued development of air pollutant prediction algorithms is critical for mitigating the harmful effects of air pollution on human health and the environment.

Although a lot of work was carried out for the prediction of air quality [88], as previous literature showed, our study used BiLSTM deep learning method that was used for air quality prediction in multiple urban cities. There are several benefits of using BiLSTM for air quality prediction as compared to other deep learning methods, such as convolutional neural networks (CNNs) or recurrent neural networks (RNNs). Firstly, BiLSTM is particularly effective in capturing temporal dependencies and patterns in time series data, which is essential for air quality prediction. BiLSTM models can effectively model long-term dependencies in the data, which can help improve the accuracy of predictions. Secondly, BiLSTM models are bidirectional, which means that they can process the input sequence in both forward and backward directions. This allows the model to consider both past and future information when making predictions, which can lead to better performance compared to unidirectional models. Additionally, BiLSTM models are capable of handling variable-length input sequences, which is important for air quality prediction, where the length of the input sequence can vary depending on the frequency of measurements. BiLSTM models are relatively simple to implement and can be trained efficiently on large datasets. This makes them a popular choice for air quality prediction, where large amounts of data are often available. Overall, the benefits of using BiLSTM for air quality prediction include its ability to capture temporal dependencies, bidirectional processing, handling of variable-length input sequences, and efficient training on large datasets. These advantages make BiLSTM a promising deep learn-

ing method for air quality prediction. Practical implications of this study lies in monitoring the air quality pattern change and prediction is helpful for government in implementing the policy for air pollution control, while theoretical contribution of this study lies in using the deep learning model in predicting air quality change, which can be helpful and motivate researcher in using latest method in future [88–90].

Air pollution prediction has both practical and theoretical implications. Some of these implications are:

4.1. Practical Implications

a. Public Health: Air pollution prediction can help in protecting public health by providing early warnings of potentially hazardous air quality conditions. This information can be used to warn vulnerable populations and limit their exposure to air pollution. It can also help policymakers to take measures to reduce pollution levels in affected areas.
b. Urban Planning: Air pollution prediction can aid in urban planning by providing accurate and timely data on air quality levels in different parts of the city. This information can help policymakers to make informed decisions regarding land-use planning and the location of industrial sites and transportation routes.
c. Industrial Operations: Air pollution prediction can be used in industrial operations to predict the impact of air pollution on the environment and the health of workers. This information can help companies to take measures to reduce their emissions and prevent environmental damage.

4.2. Theoretical Implications

a. Scientific Research: Air pollution prediction can be used to advance scientific research in the field of atmospheric science, environmental science, and public health. It can also help researchers to better understand the sources of air pollution and the factors that contribute to its formation and dispersion.
b. Policy Development: Air pollution prediction can help policymakers to develop more effective policies and regulations to reduce air pollution levels. It can also aid in the evaluation of the effectiveness of current policies and the development of new ones.
c. Climate Change: Air pollution prediction can provide valuable insights into the impact of air pollution on climate change. It can help scientists to better understand the complex interactions between air pollution and climate change and to develop strategies for mitigating the impact of air pollution on the environment.

In summary, air pollution prediction has practical implications for protecting public health, urban planning, and industrial operations, as well as theoretical implications for scientific research, policy development, and climate change.

5. Conclusions

This study proposed the deep learning method to predict the change in air quality patterns in different nearby cities and help in analysis of spatial patterns behavior in relation to environment. The benefit of prediction method is to help government in formulating a policy for prevention of this air pollution. There are several significant problems in the prevention and control of air pollution in Henan Province that are worth thinking about: the general rebound of ozone in the province, the heavy breakdown of secondary fine particulate matter, the pollution problems of heavy industrial areas and non-channel cities are prominent, the air quality in districts and counties is poor, and the level of pollution control between different regions is uneven. Although the air pollution problem is closely related to objective factors such as regional topography and meteorological conditions, it is more reflected in the environment.

This paper, however, has room for improvement. Other important aspects of pollution concentrations, such as weather and topography, are not considered in this article due

to data availability. These parameters are predicted to increase model performance and should be considered in future study. Furthermore, the experiments in this study were all based in Henan, China, and the findings may be limited to the examined area. Although the suggested technique is believed to be relevant to various locations and contaminants, further research is required to confirm its reliability and generalizability.

Furthermore, while the suggested technique delivers a better prediction for data with a higher temporal resolution, it takes longer to train. Because the base model or base-resolution data are typically bigger in size than the goal resolution. This problem can be addressed in the future. Other future possibilities for this research might include investigating the applicability of other techniques with the BLSTM model in other similar challenges. Is it feasible, for example, to transfer knowledge from another domain, such as meteorological characteristics, straight to concentrations? This might help anticipate air quality in locations where there are no monitoring stations.

There are several suggestions for policymakers and stakeholders who are working with the government:

- The first suggestion is that the steel industry in Henan Province should develop in a balanced and green way, improve industrial concentration and environmental protection law enforcement, establish a fair, competitive environment, improve the enthusiasm of enterprises to control pollution, and enterprises should consider taking the road of high-quality development from the long-term perspective of industrial transformation and source process structure adjustment.
- The second is to strengthen the standardization of provincial control stations and the non-point source control below the district and county levels and incorporate district and county sites into the urban state control assessment system, not only one city and one policy, but also one county and one policy, effectively avoiding "one size fits all" environmental management.
- The third is to promote the landing of scientific research results to support environmental management needs. The challenge of improving air quality is the "secondary pollution" treatment based on secondary $PM_{2.5}$ and ozone (O_3), and the causes of ozone in different regions, the coordinated control scheme between $PM_{2.5}$ and ozone, the proportion of VOC and NOx emission reduction, and the objective understanding of NH_3 emissions and treatment need to carry out in-depth scientific research to achieve scientific pollution control truly.

Supplementary Materials: The following supporting information can be downloaded at: https://www.mdpi.com/article/10.3390/atmos14050902/s1, Annexure Table S1: List of stations of air quality; Annexure Table S2: City wise air pollution pattern change.

Author Contributions: Conceptualization, M.A.B., Z.S., U.A.B. and N.A.; methodology, M.A.B., Z.S., U.A.B. and N.A.; software, M.A.B., Z.S., U.A.B. and N.A.; validation, M.A.B., Z.S., U.A.B. and N.A.; writing—review and editing, M.A.B., Z.S., U.A.B. and N.A.; supervision, M.A.B., Z.S., U.A.B. and N.A. All authors have read and agreed to the published version of the manuscript.

Funding: This project is supported by Natural Science Foundation of China (Grant No.42171456 and U1811464). The authors would also like to thank the Researchers Supporting Project Number (RSPD-2023R668), King Saud University, Riyadh, Saudi Arabia. Also thanks for partial funding by National key R&D project: 2020YFB2104403; Key research and development plan of the Ministry of Science and Technology: 2021ZD0111002, Hainan University Research Fund (project nos. KYQD (ZR)-22064, KYQD (ZR)-22063, and KYQD (ZR)-22065), Hainan Provincial Natural Science Foundation of China (NO. 123QN182).

Institutional Review Board Statement: Not applicable.

Informed Consent Statement: Not applicable.

Data Availability Statement: All data is available inside the manuscript.

Conflicts of Interest: The authors declare no conflict of interest.

References

1. Aamir, M.; Li, Z.; Bazai, S.; Wagan, R.A.; Bhatti, U.A.; Nizamani, M.M.; Akram, S. Spatiotemporal Change of Air-Quality Patterns in Hubei Province—A Pre- to Post-COVID-19 Analysis Using Path Analysis and Regression. *Atmosphere* **2021**, *12*, 1338. [CrossRef]
2. Li, Q.; Miao, Y.; Zeng, X.; Tarimo, C.S.; Wu, C.; Wu, J. Prevalence and factors for anxiety during the coronavirus disease 2019 (COVID-19) epidemic among the teachers in China. *J. Affect. Disord.* **2020**, *277*, 153–158. [CrossRef] [PubMed]
3. Bhatti, U.A.; Zeeshan, Z.; Nizamani, M.M.; Bazai, S.; Yu, Z.; Yuan, L. Assessing the change of ambient air quality patterns in Jiangsu Province of China pre-to post-COVID-19. *Chemosphere* **2022**, *288*, 132569. [CrossRef] [PubMed]
4. Bhatti, U.A.; Yan, Y.; Zhou, M.; Ali, S.; Hussain, A.; Qingsong, H.; Yuan, L. Time series analysis and forecasting of air pollution particulate matter (PM 2.5): An SARIMA and factor analysis approach. *IEEE Access* **2021**, *9*, 41019–41031. [CrossRef]
5. Chen, Q.X.; Huang, C.L.; Yuan, Y.; Tan, H.P. Influence of COVID-19 event on air quality and their association in Mainland China. *Aerosol Air Qual. Res.* **2020**, *20*, 1541–1551. [CrossRef]
6. Chen, W.; Tang, H.; Zhao, H. Urban air quality evaluations under two versions of the national ambient air quality standards of China. *Atmos. Pollut. Res.* **2016**, *7*, 49–57. [CrossRef]
7. Cretescu, I.; Isopescu, D.N.; Lutic, D.; Soreanu, G. Indoor air pollutants and the future perspectives for living space design. In *Indoor Environment and Health*; IntechOpen: London, UK, 2019.
8. Dai, Q.; Liu, B.; Bi, X.; Wu, J.; Liang, D.; Zhang, Y.; Hopke, P.K. Dispersion normalized PMF provides insights into the significant changes in source contributions to PM 2.5 after the COVID-19 outbreak. *Environ. Sci. Technol.* **2020**, *54*, 9917–9927. [CrossRef]
9. Donzelli, G.; Cioni, L.; Cancellieri, M.; Morales, A.L.; Suárez-Varela, M.M.M. The Effect of the COVID-19 Lockdown on Air Quality in Three Italian Medium-Sized Cities. *Atmosphere* **2020**, *11*, 1118. [CrossRef]
10. Fang, C.; Liang, L.; Wang, Z. Quantitative simulation and verification of upgrade law of sustainable development in Beijing-Tianjin-Hebei urban agglomeration. *Sci. China Earth Sci.* **2019**, *62*, 2031–2049. [CrossRef]
11. Gough, W.A.; Anderson, V. Changing Air Quality and the Ozone Weekend Effect during the COVID-19 Pandemic in Toronto, Ontario, Canada. *Climate* **2022**, *10*, 41. [CrossRef]
12. Guarnieri, M.; Balmes, J.R. Outdoor air pollution and asthma. *Lancet* **2014**, *383*, 1581–1592. [CrossRef] [PubMed]
13. Hasnain, A.; Bhatti, U.A.; Wei, G. Spatio-temporal Impact of the COVID-19 Pandemic Lockdown on Air Quality Pattern in Nanjing, China. *Front. Environ. Sci.* **2022**, *10*, 1548.
14. Hasan, N.; Toma, R.N.; Nahid, A.-A.; Islam, M.M.M.; Kim, J.-M. Electricity Theft Detection in Smart Grid Systems: A CNN-LSTM Based Approach. *Energies* **2019**, *12*, 3310. [CrossRef]
15. He, J.; Gong, S.; Yu, Y.; Yu, L.; Wu, L.; Mao, H.; Song, C.; Zhao, S.; Liu, H.; Li, X.; et al. Air pollution characteristics and their relation to meteorological conditions during 2014–2015 in major Chinese cities. *Environ. Pollut.* **2017**, *223*, 484–496. [CrossRef] [PubMed]
16. Wong, Y.J.; Yeganeh, A.; Chia, M.Y.; Shiu, H.Y.; Ooi, M.C.G.; Chang, J.H.W.; Shimizu, Y.; Ryosuke, H.; Try, S.; Elbeltagi, A. Quantification of COVID-19 impacts on NO_2 and O_3: Systematic model selection and hyperparameter optimization on AI-based meteorological-normalization methods. *Atmos. Environ.* **2023**, *301*, 119677. [CrossRef]
17. Wong, Y.J.; Shiu, H.-Y.; Chang, J.H.-H.; Ooi, M.C.G.; Li, H.-H.; Homma, R.; Shimizu, Y.; Chiueh, P.-T.; Maneechot, L.; Sulaiman, N.M.N. Spatiotemporal impact of COVID-19 on Taiwan air quality in the absence of a lockdown: Influence of urban public transportation use and meteorological conditions. *J. Clean. Prod.* **2022**, *365*, 132893. [CrossRef]
18. Naqvi, H.R.; Datta, M.; Mutreja, G.; Siddiqui, M.A.; Naqvi, D.F.; Naqvi, A.R. Improved air quality and associated mortalities in India under COVID-19 lockdown. *Environ. Pollut.* **2020**, *268*, 115691. [CrossRef]
19. Abdullah, S.; Mansor, A.A.; Napi, N.N.L.M.; Mansor, W.N.W.; Ahmed, A.N.; Ismail, M.; Ramly, Z.T.A. Air quality status during 2020 Malaysia Movement Control Order (MCO) due to 2019 novel coronavirus (2019-nCoV) pandemic. *Sci. Total Environ.* **2020**, *729*, 139022. [CrossRef]
20. Nakada, L.Y.K.; Urban, R.C. COVID-19 pandemic: Impacts on the air quality during the partial lockdown in São Paulo state, Brazil. *Sci. Total. Environ.* **2020**, *730*, 139087. [CrossRef]
21. Dang, H.-A.H.; Trinh, T.-A. Does the COVID-19 lockdown improve global air quality? New cross-national evidence on its unintended consequences. *J. Environ. Econ. Manag.* **2020**, *105*, 102401. [CrossRef]
22. Zhu, Y.; Xie, J.; Huang, F.; Cao, L. The mediating effect of air quality on the association between human mobility and COVID-19 infection in China. *Environ. Res.* **2020**, *189*, 109911. [CrossRef] [PubMed]
23. Ash'aari, Z.H.; Aris, A.Z.; Ezani, E.; Kamal, N.I.A.; Jaafar, N.; Jahaya, J.N.; Manan, S.A.; Saifuddin, M.F.U. Spatiotemporal Variations and Contributing Factors of Air Pollutant Concentrations in Malaysia during Movement Control Order due to Pandemic COVID-19. *Aerosol Air Qual. Res.* **2020**, *20*, 2047–2061. [CrossRef]
24. Rudke, A.; Martins, J.; de Almeida, D.; Martins, L.; Beal, A.; Hallak, R.; Freitas, E.; Andrade, M.; Foroutan, H.; Baek, B.; et al. How mobility restrictions policy and atmospheric conditions impacted air quality in the State of São Paulo during the COVID-19 outbreak. *Environ. Res.* **2021**, *198*, 111255. [CrossRef] [PubMed]
25. Archer, C.L.; Cervone, G.; Golbazi, M.; Al Fahel, N.; Hultquist, C. Changes in air quality and human mobility in the USA during the COVID-19 pandemic. *Bull. Atmos. Sci. Technol.* **2020**, *1*, 491–514. [CrossRef]
26. Gualtieri, G.; Brilli, L.; Carotenuto, F.; Vagnoli, C.; Zaldei, A.; Gioli, B. Quantifying road traffic impact on air quality in urban areas: A Covid19-induced lockdown analysis in Italy. *Environ. Pollut.* **2020**, *267*, 115682. [CrossRef]

27. Wang, Y.-N.; Wang, Q.; Li, Y.; Wang, H.; Gao, Y.; Sun, Y.; Wang, B.; Bian, R.; Li, W.; Zhan, M. Impact of incineration slag co-disposed with municipal solid waste on methane production and methanogens ecology in landfills. *Bioresour. Technol.* **2023**, *377*, 128978. [CrossRef]
28. Hu, J.; Ying, Q.; Wang, Y.; Zhang, H. Characterizing multi-pollutant air pollution in China: Comparison of three air quality indices. *Environ. Int.* **2015**, *84*, 17–25. [CrossRef]
29. Jakob, A.; Hasibuan, S.; Fiantis, D. Empirical evidence shows that air quality changes during COVID-19 pandemic lockdown in Jakarta, Indonesia are due to seasonal variation, not restricted movements. *Environ. Res.* **2022**, *208*, 112391. [CrossRef]
30. Jakovljević, I.; Štrukil, Z.S.; Godec, R.; Davila, S.; Pehnec, G. Influence of lockdown caused by the COVID-19 pandemic on air pollution and carcinogenic content of particulate matter observed in Croatia. *Air Qual. Atmos. Health* **2021**, *14*, 467–472. [CrossRef]
31. Jeong, C.-H.; Yousif, M.; Evans, G.J. Impact of the COVID-19 lockdown on the chemical composition and sources of urban PM2.5. *Environ. Pollut.* **2022**, *292*, 118417. [CrossRef]
32. Karagulian, F.; Temimi, M.; Ghebreyesus, D.; Weston, M.; Kondapalli, N.K.; Valappil, V.K.; Aldababesh, A.; Lyapustin, A.; Chaouch, N.; Al Hammadi, F.; et al. Analysis of a severe dust storm and its impact on air quality conditions using WRF-Chem modeling, satellite imagery, and ground observations. *Air Qual. Atmos. Health* **2019**, *12*, 453–470. [CrossRef]
33. Lai, X.; Li, H.; Pan, Y. A combined model based on feature selection and support vector machine for PM 2.5 prediction. *J. Intell. Fuzzy Syst.* **2021**, *40*, 10099–10113. [CrossRef]
34. Li, J.; Chen, Z.; Nie, Y.; Ma, Y.; Guo, Q.; Dai, X. Identification of Symptoms Prognostic of COVID-19 Severity: Multivariate Data Analysis of a Case Series in Henan Province. *J. Med. Internet Res.* **2020**, *22*, e19636. [CrossRef] [PubMed]
35. Wu, X.; Liu, Z.; Yin, L.; Zheng, W.; Song, L.; Tian, J.; Yang, B.; Liu, S. A Haze Prediction Model in Chengdu Based on LSTM. *Atmosphere* **2021**, *12*, 1479. [CrossRef]
36. Li, L.; Li, Q.; Huang, L.; Wang, Q.; Zhu, A.; Xu, J.; Liu, Z.; Li, H.; Shi, L.; Li, R.; et al. Air quality changes during the COVID-19 lockdown over the Yangtze River Delta Region: An insight into the impact of human activity pattern changes on air pollution variation. *Sci. Total Environ.* **2020**, *732*, 139282. [CrossRef]
37. Lian, X.; Huang, J.; Huang, R.; Liu, C.; Wang, L.; Zhang, T. Impact of city lockdown on the air quality of COVID-19-hit of Wuhan city. *Sci. Total Environ.* **2020**, *742*, 140556. [CrossRef]
38. Liang, X.M.; Chen, L.G.; Shen, G.F.; Lu, Q.; Liu, M.; Lu, H.T.; Tao, S. Volatile Organic Compounds (VOCs) Emission Inventory from Domestic Sources in China. *Huan Jing Ke Xue Huanjing Kexue* **2021**, *42*, 5162–5168.
39. Statistical Yearbook of Henan. 2018. Available online: https://www.chinayearbooks.com/tags/henan-statistical-yearbook (accessed on 1 December 2022).
40. Lin, G.-Y.; Lee, Y.-M.; Tsai, C.-J.; Lin, C.-Y. Spatial-temporal characterization of air pollutants using a hybrid deep learning/Kriging model incorporated with a weather normalization technique. *Atmos. Environ.* **2022**, *289*, 119304. [CrossRef]
41. China National Environmental Monitoring Centre. Available online: http://www.cnemc.cn (accessed on 1 December 2022).
42. Liu, B.; Jin, Y.; Li, C. Analysis and prediction of air quality in Nanjing from autumn 2018 to summer 2019 using PCR–SVR–ARMA combined model. *Sci. Rep.* **2021**, *11*, 348. [CrossRef]
43. Liu, S.; Hua, S.; Wang, K.; Qiu, P.; Liu, H.; Wu, B.; Shao, P.; Liu, X.; Wu, Y.; Xue, Y.; et al. Spatial-temporal variation characteristics of air pollution in Henan of China: Localized emission inventory, WRF/Chem simulations and potential source contribution analysis. *Sci. Total Environ.* **2018**, *624*, 396–406. [CrossRef]
44. Farzad, A.; Mashayekhi, H.; Hassanpour, H. A comparative performance analysis of different activation functions in LSTM networks for classification. *Neural Comput. Appl.* **2019**, *31*, 2507–2521. [CrossRef]
45. Vijayaprabakaran, K.; Sathiyamurthy, K. Towards activation function search for long short-term model network: A differential evolution based approach. *J. King Saud Univ. Comput. Inf. Sci.* **2022**, *34*, 2637–2650.
46. Brogärd, A.; Song, P. Performance Analysis of Various Activation Functions Using LSTM Neural Network for Movie Recommendation Systems. Degree Project Technology. In *First Cycle*; Diva-Portal: Stockholm, Sweden, 2020.
47. Liu, T.; Wang, X.; Hu, J.; Wang, Q.; An, J.; Gong, K.; Sun, J.; Li, L.; Qin, M.; Li, J.; et al. Driving Forces of Changes in Air Quality during the COVID-19 Lockdown Period in the Yangtze River Delta Region, China. *Environ. Sci. Technol. Lett.* **2020**, *7*, 779–786. [CrossRef]
48. Pang, N.; Gao, J.; Zhao, P.; Wang, Y.; Xu, Z.; Chai, F. The impact of fireworks control on air quality in four Northern Chinese cities during the Spring Festival. *Atmos. Environ.* **2021**, *244*, 117958. [CrossRef]
49. Putaud, J.-P.; Pozzoli, L.; Pisoni, E.; Dos Santos, S.M.; Lagler, F.; Lanzani, G.; Santo, U.D.; Colette, A. Impacts of the COVID-19 lockdown on air pollution at regional and urban background sites in northern Italy. *Atmos. Chem. Phys. Discuss.* **2021**, *21*, 7597–7609. [CrossRef]
50. Shen, F.; Ge, X.; Hu, J.; Nie, D.; Tian, L.; Chen, M. Air pollution characteristics and health risks in Henan Province, China. *Environ. Res.* **2017**, *156*, 625–634. [CrossRef]
51. Mao, M.; Sun, H.; Zhang, X. Air pollution characteristics and health risks in the Yangtze river economic belt, China during winter. *Int. J. Environ. Res. Public Health* **2020**, *17*, 9172. [CrossRef]
52. Sicard, P.; De Marco, A.; Agathokleous, E.; Feng, Z.; Xu, X.; Paoletti, E.; Rodriguez, J.J.D.; Calatayud, V. Amplified ozone pollution in cities during the COVID-19 lockdown. *Sci. Total Environ.* **2020**, *735*, 139542. [CrossRef]
53. Siciliano, B.; Dantas, G.; da Silva, C.M.; Arbilla, G. Increased ozone levels during the COVID-19 lockdown: Analysis for the city of Rio de Janeiro, Brazil. *Sci. Total Environ.* **2020**, *737*, 139765. [CrossRef]

54. Sohrabi, C.; Alsafi, Z.; O'Neill, N.; Khan, M.; Kerwan, A.; Al-Jabir, A.; Iosifidis, C.; Agha, R. World Health Organization declares global emergency: A review of the 2019 novel coronavirus (COVID-19). *Int. J. Surg.* **2020**, *76*, 71–76. [CrossRef]
55. Song, Y.; Li, Z.; Liu, J.; Yang, T.; Zhang, M.; Pang, J. The effect of environmental regulation on air quality in China: A natural experiment during the COVID-19 pandemic. *Atmos. Pollut. Res.* **2021**, *12*, 21–30. [CrossRef]
56. Swamy, Y.; Venkanna, R.; Nikhil, G.; Chitanya, D.; Sinha, P.R.; Ramakrishna, M.; Rao, A. Impact of Nitrogen Oxides, Volatile Organic Compounds and Black Carbon on Atmospheric Ozone Levels at a Semi Arid Urban Site in Hyderabad. *Aerosol Air Qual. Res.* **2012**, *12*, 662–671. [CrossRef]
57. Thakur, A.K.; Sathyamurthy, R.; Ramalingam, V.; Lynch, I.; Sharshir, S.W.; Ma, Z.; Poongavanam, G.; Lee, S.; Jeong, Y.; Hwang, J.-Y. A case study of SARS-CoV-2 transmission behavior in a severely air-polluted city (Delhi, India) and the potential usage of graphene based materials for filtering air-pollutants and controlling/monitoring the COVID-19 pandemic. *Environ. Sci. Process. Impacts* **2021**, *23*, 923–946. [CrossRef] [PubMed]
58. Tello-Leal, E.; Macías-Hernández, B.A. Association of environmental and meteorological factors on the spread of COVID-19 in Victoria, Mexico, and air quality during the lockdown. *Environ. Res.* **2021**, *196*, 110442. [CrossRef]
59. Vallyathan, V.; Shi, X. The role of oxygen free radicals in occupational and environmental lung diseases. *Environ. Health Perspect.* **1997**, *105* (Suppl. 1), 165–177.
60. Wang, T.; Nie, W.; Gao, J.; Xue, L.K.; Gao, X.M.; Wang, X.F.; Qiu, J.; Poon, C.N.; Meinardi, S.; Blake, D.; et al. Air quality during the 2008 Beijing Olympics: Secondary pollutants and regional impact. *Atmos. Meas. Tech.* **2010**, *10*, 7603–7615. [CrossRef]
61. Wan, S.; Cui, K.; Wang, Y.-F.; Wu, J.-L.; Huang, W.-S.; Xu, K.; Zhang, J. Impact of the COVID-19 Event on Trip Intensity and Air Quality in Southern China. *Aerosol Air Qual. Res.* **2020**, *20*, 1727–1747. [CrossRef]
62. Weather and Air Quality Website. Available online: www.tianqihoubao.com (accessed on 27 September 2022).
63. Wetchayont, P.; Hayasaka, T.; Khatri, P. Air Quality Improvement during COVID-19 Lockdown in Bangkok Metropolitan, Thailand: Effect of the Long-range Transport of Air Pollutants. *Aerosol Air Qual. Res.* **2021**, *21*, 200662. [CrossRef]
64. Yang, Z.; Zeng, Z.; Wang, K.; Wong, S.-S.; Liang, W.; Zanin, M.; Liu, P.; Cao, X.; Gao, Z.; Mai, Z.; et al. Modified SEIR and AI prediction of the epidemics trend of COVID-19 in China under public health interventions. *J. Thorac. Dis.* **2020**, *12*, 165–174. [CrossRef]
65. Zeng, J.; Liu, T.; Feiock, R.; Li, F. The impacts of China's provincial energy policies on major air pollutants: A spatial econometric analysis. *Energy Policy* **2019**, *132*, 392–403. [CrossRef]
66. Zhao, J.; Gao, H.Y.; Feng, Z.Y.; Wu, Q.J. A retrospective analysis of the clinical and epidemiological characteristics of COVID-19 patients in Henan Provincial People's Hospital, Zhengzhou, China. *Front. Med.* **2020**, *7*, 286. [CrossRef] [PubMed]
67. Zhang, J.; Cui, K.; Wang, Y.-F.; Wu, J.-L.; Huang, W.-S.; Wan, S.; Xu, K. Temporal Variations in the Air Quality Index and the Impact of the COVID-19 Event on Air Quality in Western China. *Aerosol Air Qual. Res.* **2020**, *20*, 1552–1568. [CrossRef]
68. Liu, Y.; Tian, J.; Zheng, W.; Yin, L. Spatial and temporal distribution characteristics of haze and pollution particles in China based on spatial statistics. *Urban Clim.* **2021**, *41*, 101031. [CrossRef]
69. Yin, L.; Wang, L.; Huang, W.; Liu, S.; Yang, B.; Zheng, W. Spatiotemporal Analysis of Haze in Beijing Based on the Multi-Convolution Model. *Atmosphere* **2021**, *12*, 1408. [CrossRef]
70. Shang, K.; Chen, Z.; Liu, Z.; Song, L.; Zheng, W.; Yang, B.; Liu, S.; Yin, L. Haze Prediction Model Using Deep Recurrent Neural Network. *Atmosphere* **2021**, *12*, 1625. [CrossRef]
71. Bai, X.; Zhang, S.; Li, C.; Xiong, L.; Song, F.; Du, C.; Li, M.; Luo, Q.; Xue, Y.; Wang, S. A carbon-neutrality-capactiy index for evaluating carbon sink contributions. *Environ. Sci. Ecotechnology* **2023**, *15*, 100237. [CrossRef]
72. Bhatti, U.A.; Hashmi, M.Z.; Sun, Y.; Masud, M.; Nizamani, M.M. Artificial intelligence applications in reduction of carbon emissions: Step towards sustainable environment. *Front. Environ. Sci.* **2023**, *11*, 1183620. [CrossRef]
73. Miao, L.; Tang, S.; Ren, Y.; Kwan, M.-P.; Zhang, K. Estimation of daily ground-level PM2.5 concentrations over the Pearl River Delta using 1 km resolution MODIS AOD based on multi-feature BiLSTM. *Atmos. Environ.* **2022**, *290*, 1193620. [CrossRef]
74. Rodríguez-Urrego, D.; Rodríguez-Urrego, L. Air quality during the COVID-19: PM2.5 analysis in the 50 most polluted capital cities in the world. *Environ. Pollut.* **2020**, *266*, 115042. [CrossRef]
75. Tobías, A.; Carnerero, C.; Reche, C.; Massagué, J.; Via, M.; Minguillón, M.C.; Alastuey, A.; Querol, X. Changes in air quality during the lockdown in Barcelona (Spain) one month into the SARS-CoV-2 epidemic. *Sci. Total Environ.* **2020**, *726*, 138540. [CrossRef]
76. Mueller, S.F.; Mallard, J.W. Contributions of natural emissions to ozone and pm 2.5 as simulated by the community multiscale air quality (cmaq) model. *Environ. Sci. Technol.* **2011**, *45*, 4817–4823. [CrossRef] [PubMed]
77. Wang, P.; Wang, P.; Chen, K.; Du, J.; Zhang, H. Ground-level ozone simulation using ensemble WRF/Chem predictions over the Southeast United States. *Chemosphere* **2021**, *287*, 132428. [CrossRef] [PubMed]
78. Wang, Z.; Maeda, T.; Hayashi, M.; Hsiao, L.-F.; Liu, K.-Y. A Nested Air Quality Prediction Modeling System for Urban and Regional Scales: Application for High-Ozone Episode in Taiwan. *Water Air Soil Pollut.* **2001**, *130*, 391–396. [CrossRef]
79. Konopka, P.; Grooß, J.-U.; Günther, G.; Ploeger, F.; Pommrich, R.; Müller, R.; Livesey, N. Annual cycle of ozone at and above the tropical tropopause: Observations versus simulations with the Chemical Lagrangian Model of the Stratosphere (CLaMS). *Atmos. Meas. Tech.* **2010**, *10*, 121–132. [CrossRef]
80. Wang, Y.; Lu, C.; Niu, S.; Lv, J.; Jia, X.; Xu, X.; Xue, Y.; Zhu, L.; Yan, S. Diverse Dispersion Effects and Parameterization of Relative Dispersion in Urban Fog in Eastern China. *J. Geophys. Res. Atmos.* **2023**, *128*, e2022JD037514. [CrossRef]
81. Bai, L.; Wang, J.; Ma, X.; Lu, H. Air Pollution Forecasts: An Overview. *Int. J. Environ. Res. Public Health* **2018**, *15*, 780. [CrossRef]

82. Masih, A. Machine learning algorithms in air quality modelling. *Glob. J. Environ. Sci. Manag.* **2019**, *5*, 515–534.
83. Cabaneros, S.M.; Calautit, J.K.; Hughes, B.R. A review of artificial neural network models for ambient air pollution prediction. *Environ. Model. Softw.* **2019**, *119*, 285–304. [CrossRef]
84. Liao, Q.; Zhu, M.; Wu, L.; Pan, X.; Tang, X.; Wang, Z. Deep Learning for Air Quality Forecasts: A Review. *Curr. Pollut. Rep.* **2020**, *6*, 399–409. [CrossRef]
85. Masood, A.; Ahmad, K. A review on emerging artificial intelligence (AI) techniques for air pollution forecasting: Fundamentals, application and performance. *J. Clean. Prod.* **2021**, *322*, 129072. [CrossRef]
86. Liu, H.; Yan, G.; Duan, Z.; Chen, C. Intelligent modeling strategies for forecasting air quality time series: A review. *Appl. Soft Comput.* **2021**, *102*, 106957. [CrossRef]
87. Assael, M.J.; Delaki, M.; Kakosimos, K.E. Applying the ospm model to the calculation of pm10 concentration levels in the historical centre of the city of the ssaloniki. *Atmos. Environ.* **2008**, *42*, 65–77. [CrossRef]
88. Xu, D.; Zhu, D.; Deng, Y.; Sun, Q.; Ma, J.; Liu, F. Evaluation and empirical study of Happy River on the basis of AHP: A case study of Shaoxing City (Zhejiang, China). *Mar. Freshw. Res.* **2023**, *1*, MF22196. [CrossRef]
89. Wang, Y.; Henning, S.; Poulain, L.; Lu, C.; Stratmann, F.; Wang, Y.; Niu, S.; Pöhlker, M.L.; Herrmann, H.; Wiedensohler, A. Aerosol activation characteristics and prediction at the central European ACTRIS research station of Melpitz, Germany. *Atmos. Meas. Tech.* **2022**, *22*, 15943–15962. [CrossRef]
90. Chuang, M.T.; Zhang, Y.; Kang, D. Application of wrf/chem-madrid for real-time air quality forecasting over the south eastern United States. *Atmos. Environ.* **2011**, *45*, 6241–6250. [CrossRef]